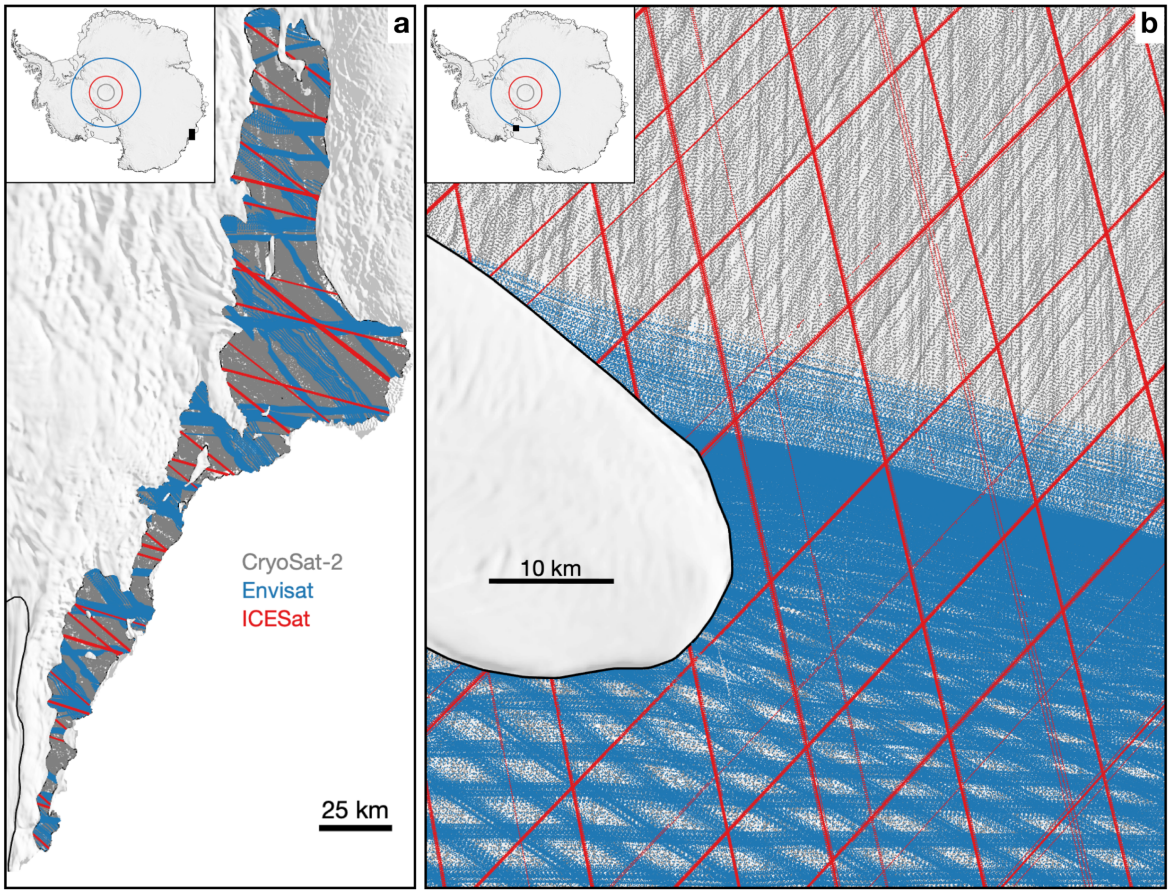


**Supplementary Figure 1: Spatial sampling of satellite laser and radar altimeters.** Spatial sampling of heights measured using CryoSat-2 (2010–present), Envisat (2002–2012), and ICESat (2003–2009) altimetry over (a) Totten Ice Shelf, East Antarctica, and (b) Ross Ice Shelf. The southern orbit limit of Envisat is visible in (b), and the orbit limits for the three altimeters are shown in the inset figures, with locations of each site shown by the black box. Some Envisat tracks sampled areas slightly south of its nominal orbit limit (81.5°S) during Phase 3 from 2010 until the end of its mission in 2012.

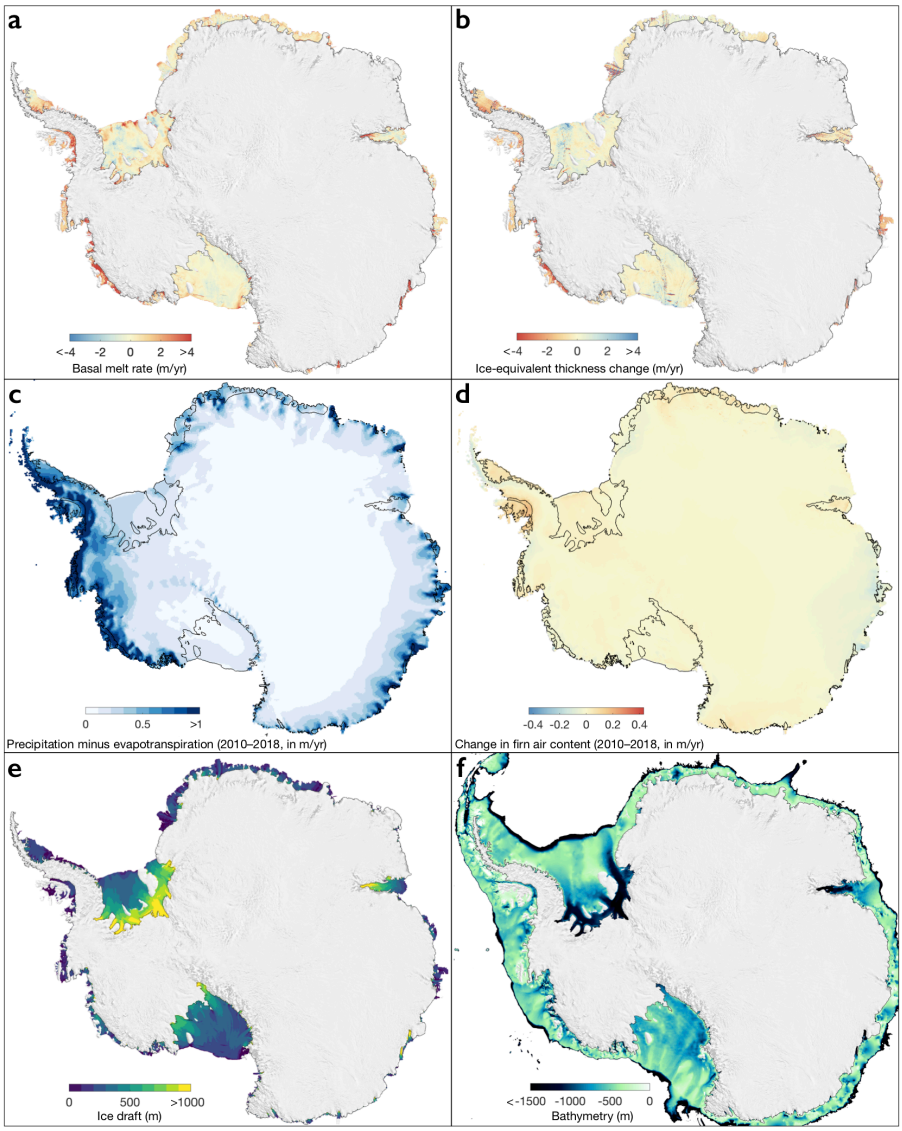


**Supplementary Figure 2: Key ice observations across Antarctic ice shelves.** Panels (a–e) are for the CryoSat-2 (2010–2018) period. (a) High resolution ice shelf basal melt rates in m of ice equivalent per year (same values as Figure 1, with a different color scale); (b) ice-equivalent thickness change in m of ice equivalent per year; (c) precipitation minus evapotranspiration in m of ice equivalent per year; (d) change in firn air content in m of air per year; (e) ice draft from CryoSat-2 with data gaps filled in using BedMachine[67]; and (f) bathymetry around Antarctica from BedMachine. Color range for (d) is scaled to be consistent with the scale for (a,b) after hydrostatic adjustment (red values indicate a positive change in firn air content).

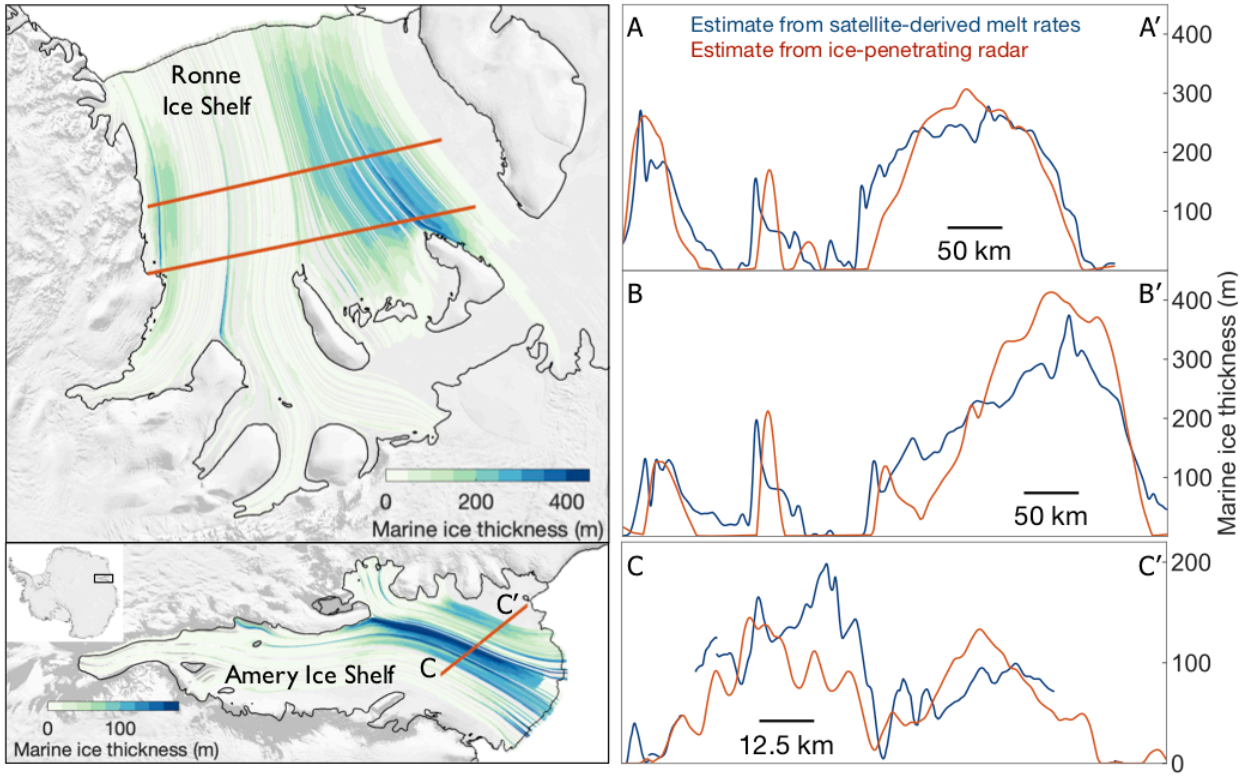


**Supplementary Figure 3: Estimates of marine-ice thickness.** Marine-ice thickness under Ronne and Amery ice shelves estimated using satellite-derived steady-state basal melt rates (left) using the methodology of ref. [83] described in Section S7. We used bicubic interpolation to extract values along three profiles (A-A', B-B', C-C') to compare them against independent estimates from airborne radar sounding from refs. [84,85].

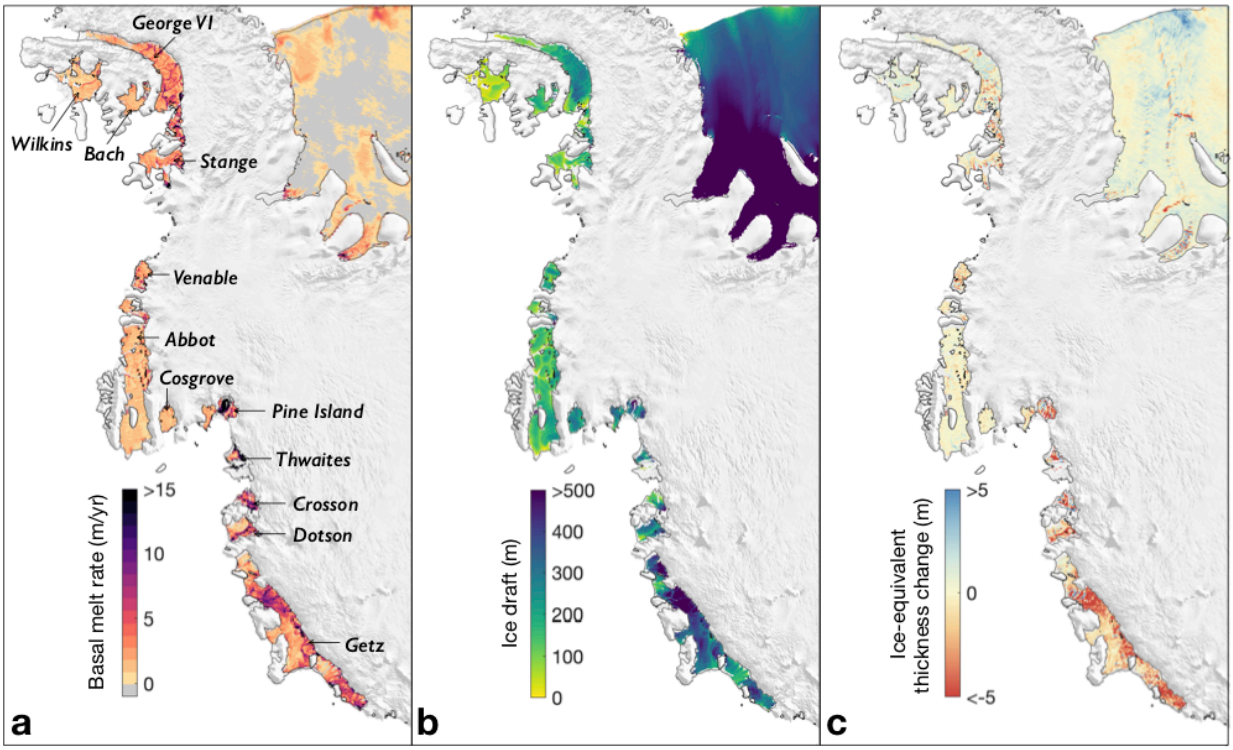


**Supplementary Figure 4: Key ice observations of Amundsen and Bellingshausen Sea ice shelves.** Amundsen Sea and Bellingshausen Sea ice shelf (a) basal melt rates in m of ice equivalent per year, (b) ice draft, and (c) thickness change in m of ice equivalent per year for the CryoSat-2 period (2010–2018). Individual ice shelves are identified on panel (a).

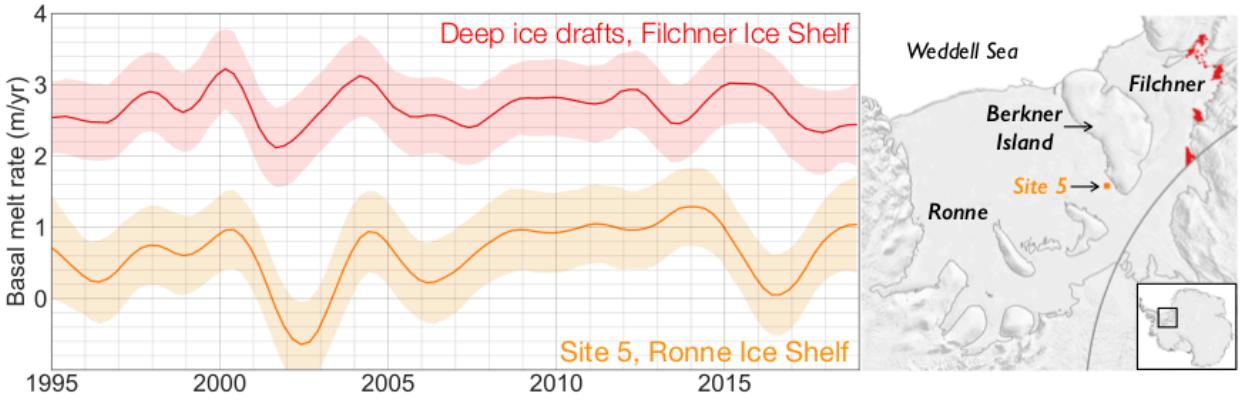


**Supplementary Figure 5: Basal melt rates at Site 5.** Basal melt rates at deep ice drafts for Filchner Ice Shelf and at observation Site 5 near the southwestern Berkner Island coast of Ronne Ice Shelf. Temporal variations of basal melting in both regions are influenced by processes in the Weddell Sea north of the ice shelves, but are not directly linked[40]. Time series are smoothed with a low-pass filter with a three-year cutoff.

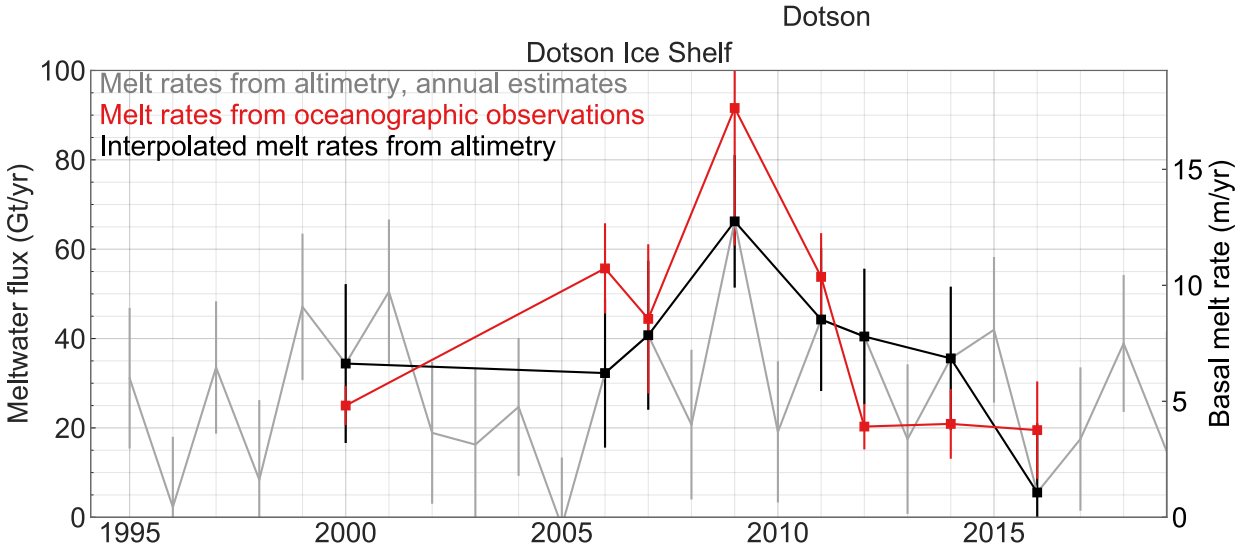


**Supplementary Figure 6: Basal melt rates for Dotson Ice Shelf.** Satellite-derived annual basal melt rates (in gray) for Dotson Ice Shelf (see Figure S4a for location) from this study compared to estimates from eight oceanographic sections near the ice front (in red)[4]. To aid visual comparison, we interpolated (in black) the raw time series to the timestamps of the oceanographic measurements.

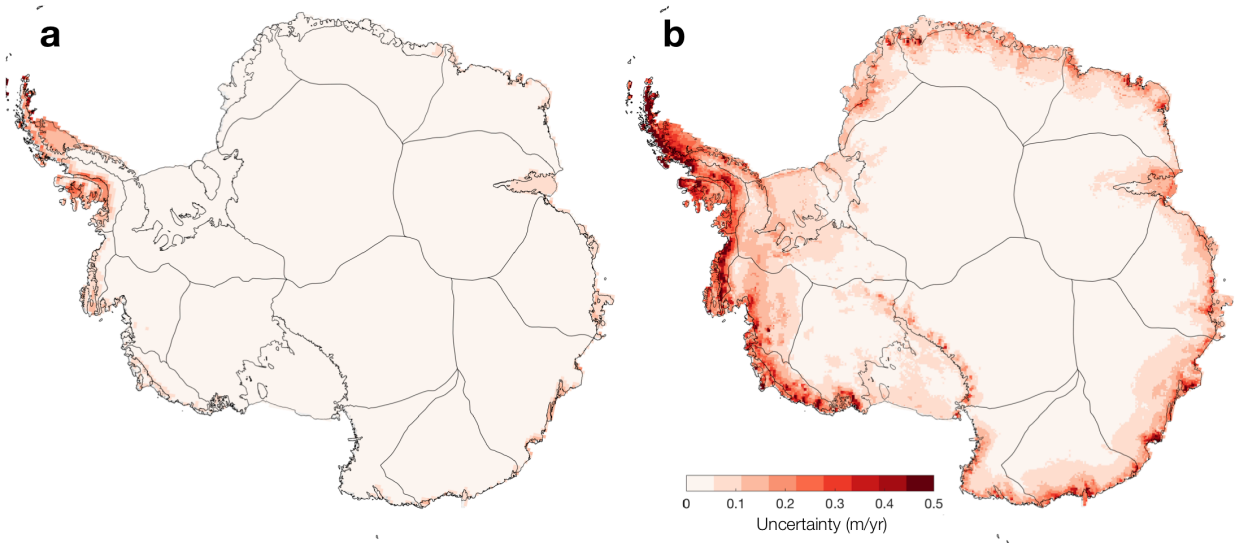


**Supplementary Figure 7: Uncertainties in changes in firn air content.** Uncertainties in changes in firn air content in m of firn air per year at annual time scales. (a) Uncertainty from steady-state assumption in climate for firn model spin-up[1]. (b) Uncertainty arising from resolution and errors in model physics, estimated as the differences between the outputs from the GSFC-FDMv0 (forced by the MERRA-2 atmospheric model with mean climate from the M2R12K replay) and the IMAU firn densification model forced by the RACMO2.3p2 regional atmospheric model[82]. Grounded-ice basins are from ref. [91]. These uncertainties represent an upper bound and are lower at the longer time scales typically considered in this study.

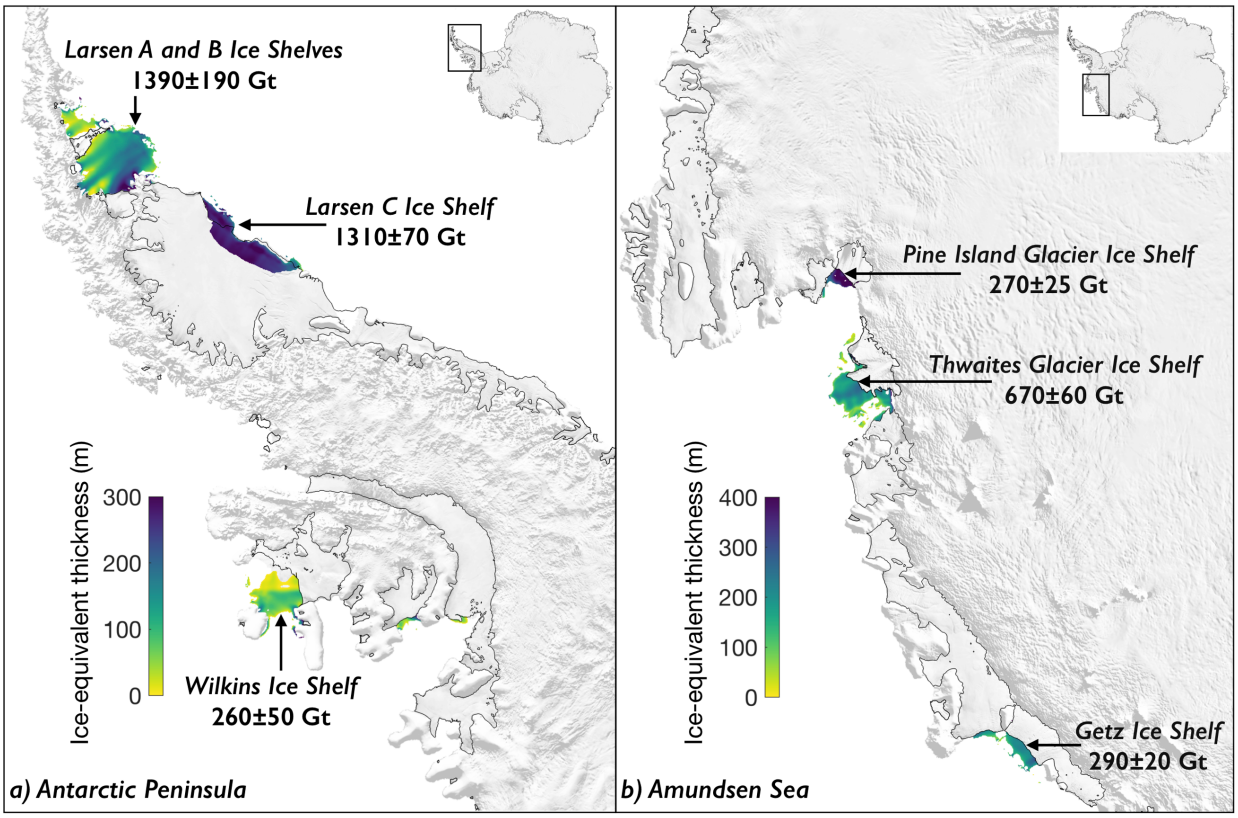


**Supplementary Figure 8: Changes in extent of Antarctic Peninsula and Amundsen Sea sector ice shelves. 1994–2018.** Ice-equivalent thickness data from the ERS-1 geodetic phase (1994/1995) are shown for regions that were covered by open ocean or sea ice at any time during the CryoSat-2 period. We only show regions with heights above mean sea level greater than 10 m (Figure 1).

| Ice Shelf | Area (km$^2$) | Latitude | Longitude | Basal melt rate, 1994–2018 (m/yr) | Meltwater flux, 1994–2018 (Gt/yr) | Excess meltwater flux, 1994–2018 (Gt/yr) | Meltwater flux, 2010–2018 (Gt/yr) |
|---|---|---|---|---|---|---|---|
| George VI | 22755 | -72.39 | -70.24 | 4.3 ± 2.2 | 88.8 ± 45.7 | 16.4 ± 45.7 | 82.4 ± 45.7 |
| Bach | 4444 | -72.05 | -71.82 | 3.2 ± 2.1 | 13.1 ± 8.5 | 3.2 ± 8.5 | 11.8 ± 8.5 |
| Wilkins | 10390 | -70.40 | -71.73 | 2.7 ± 3.4 | 26.1 ± 32.0 | 2.5 ± 32.0 | 23.2 ± 32.0 |
| Stange | 7397 | -73.29 | -76.64 | 3.7 ± 2.1 | 25.4 ± 14.2 | 7.2 ± 14.2 | 25.9 ± 14.2 |
| Venable | 3037 | -73.11 | -87.33 | 5.1 ± 2.0 | 14.3 ± 5.5 | 7.6 ± 5.6 | 10.3 ± 5.5 |
| Abbot | 27461 | -72.94 | -94.78 | 1.5 ± 1.5 | 37.1 ± 38.1 | 8.5 ± 38.1 | 37.9 ± 38.2 |
| **Bellingshausen** | **75484** | **–** | **–** | **3.0 ± 1.0** | **204.8 ± 69.7** | **45.3 ± 69.7** | **191.4 ± 69.7** |
| Cosgrove | 2964 | -73.56 | -100.33 | 1.0 ± 1.5 | 2.7 ± 4.1 | 0.0 ± 4.1 | 4.2 ± 4.1 |
| Pine Island | 5950 | -74.83 | -100.79 | 14.0 ± 1.6 | 76.6 ± 8.6 | 15.8 ± 8.6 | 76.0 ± 8.7 |
| Thwaites | 3352 | -75.08 | -106.16 | 26.7 ± 2.4 | 81.9 ± 7.4 | 11.6 ± 7.4 | 81.1 ± 7.4 |
| Crosson | 2932 | -75.03 | -110.51 | 7.8 ± 1.8 | 20.9 ± 4.9 | 10.8 ± 4.9 | 17.9 ± 4.9 |
| Dotson | 5657 | -74.70 | -112.92 | 5.4 ± 1.6 | 28.2 ± 8.5 | 13.6 ± 8.5 | 26.1 ± 8.5 |
| Getz | 32114 | -74.46 | -124.49 | 4.2 ± 1.4 | 124.1 ± 40.9 | 61.4 ± 40.9 | 122.6 ± 40.9 |
| **Amundsen** | **52969** | **–** | **–** | **6.9 ± 0.9** | **334.5 ± 43.7** | **113.2 ± 43.7** | **327.9 ± 43.8** |
| Land | 587 | -75.58 | -141.43 | 20.4 ± 2.7 | 11.0 ± 1.5 | 2.3 ± 1.5 | 10.9 ± 1.5 |
| Nickerson | 6001 | -75.81 | -145.84 | 1.2 ± 1.4 | 6.5 ± 7.9 | -0.1 ± 7.9 | 8.0 ± 7.9 |
| Sulzberger | 11229 | -77.08 | -148.58 | 1.5 ± 1.3 | 15.7 ± 13.3 | 1.6 ± 13.3 | 18.5 ± 13.3 |
| Withrow | 341 | -77.15 | -157.17 | 3.3 ± 1.8 | 1.0 ± 0.6 | 0.0 ± 0.6 | 0.9 ± 0.6 |
| Ross West | 198293 | -80.37 | -160.13 | 0.3 ± 0.4 | 45.8 ± 68.3 | -32.4 ± 68.3 | 26.6 ± 69.2 |
| Ross East | 135261 | -80.70 | 168.59 | 0.3 ± 0.4 | 34.3 ± 45.2 | -40.2 ± 45.2 | 31.0 ± 45.3 |
| Drygalski | 2168 | -75.38 | 163.16 | 1.9 ± 0.9 | 3.8 ± 1.7 | 0.5 ± 1.7 | 3.8 ± 1.7 |
| Nansen | 1835 | -74.86 | 163.15 | 1.6 ± 1.1 | 2.8 ± 1.8 | -0.3 ± 1.8 | 2.2 ± 1.8 |
| Mariner | 2354 | -73.32 | 168.09 | 1.1 ± 1.7 | 2.3 ± 3.6 | -0.3 ± 3.6 | 2.4 ± 3.6 |
| **Ross** | **358068** | **–** | **–** | **0.4 ± 0.3** | **123.3 ± 83.5** | **-68.7 ± 83.5** | **104.3 ± 84.2** |
| Moscow University | 4145 | -66.88 | 121.07 | 7.4 ± 2.1 | 28.3 ± 8.0 | 3.8 ± 8.0 | 25.8 ± 8.0 |
| Rennick | 3123 | -70.61 | 161.69 | 1.9 ± 1.4 | 5.5 ± 3.9 | 1.3 ± 3.9 | 5.7 ± 3.9 |
| Cook | 3408 | -68.54 | 152.78 | 1.3 ± 1.6 | 3.9 ± 5.1 | -1.0 ± 5.1 | 4.6 ± 5.1 |
| Mertz | 3243 | -67.30 | 145.19 | 5.0 ± 2.4 | 14.8 ± 7.1 | 1.2 ± 7.1 | 13.8 ± 7.1 |
| Holmes | 1717 | -66.76 | 127.26 | 13.3 ± 2.9 | 20.9 ± 4.5 | 0.6 ± 4.5 | 17.7 ± 4.5 |
| Totten | 6078 | -67.05 | 116.12 | 11.5 ± 2.0 | 64.0 ± 11.0 | 8.4 ± 11.0 | 59.4 ± 11.0 |
| Shackleton | 26182 | -66.06 | 97.90 | 1.8 ± 1.9 | 44.0 ± 44.8 | 12.8 ± 44.8 | 40.7 ± 44.8 |
| West | 15306 | -66.96 | 85.00 | 1.4 ± 1.8 | 20.1 ± 25.1 | 2.9 ± 25.1 | 15.7 ± 25.1 |
| **Wilkes** | **63202** | **–** | **–** | **3.5 ± 0.9** | **201.4 ± 54.1** | **30.0 ± 54.1** | **183.5 ± 54.1** |
| **Amery** | **60228** | **–** | **–** | **0.8 ± 0.7** | **45.6 ± 40.0** | **-2.5 ± 40.0** | **48.9 ± 39.9** |
| Prince Harald | 4067 | -69.24 | 35.25 | 2.3 ± 1.9 | 8.6 ± 7.2 | 0.1 ± 7.2 | 7.4 ± 7.1 |
| Brunt_Stancomb | 34573 | -75.10 | -22.51 | 0.6 ± 0.8 | 18.0 ± 24.6 | 0.2 ± 24.6 | 17.3 ± 24.7 |
| Riiser-Larsen | 42644 | -72.91 | -15.31 | 0.5 ± 0.8 | 19.4 ± 30.0 | 3.2 ± 30.0 | 16.2 ± 30.0 |
| Quar | 2076 | -71.20 | -10.86 | 0.4 ± 0.8 | 0.7 ± 1.6 | 0.2 ± 1.6 | 0.9 ± 1.6 |
| Ekstrom | 6754 | -71.05 | -8.55 | 1.0 ± 1.2 | 6.4 ± 7.2 | 1.0 ± 7.2 | 6.4 ± 7.2 |
| Baudouin | 32789 | -69.96 | 28.47 | 1.0 ± 1.0 | 28.8 ± 29.1 | 0.8 ± 29.1 | 34.5 ± 29.1 |
| Borchgrevink | 21368 | -70.32 | 20.38 | 0.8 ± 1.0 | 15.5 ± 20.3 | 3.0 ± 20.3 | 14.4 ± 20.3 |
| Lazarev | 8456 | -69.92 | 14.45 | 0.8 ± 0.8 | 6.3 ± 6.2 | 1.9 ± 6.2 | 7.4 ± 6.3 |
| Fimbul | 40600 | -70.57 | 1.55 | 1.0 ± 0.8 | 36.2 ± 29.0 | -0.5 ± 29.0 | 32.7 ± 29.1 |
| Nivl | 7275 | -70.25 | 11.29 | 1.1 ± 1.1 | 7.0 ± 7.2 | 0.6 ± 7.2 | 7.4 ± 7.2 |
| Vigrid | 2071 | -70.23 | 8.33 | 1.2 ± 1.0 | 2.3 ± 1.8 | 0.2 ± 1.8 | 2.3 ± 1.9 |
| Atka | 1780 | -70.61 | -6.84 | 1.0 ± 1.2 | 1.6 ± 1.9 | 0.3 ± 1.9 | 1.5 ± 1.9 |
| Jelbart | 10756 | -70.97 | -4.33 | 1.0 ± 1.1 | 9.9 ± 11.3 | 1.6 ± 11.3 | 9.9 ± 11.3 |
| **Queen Maud** | **215208** | **–** | **–** | **0.8 ± 0.3** | **160.7 ± 62.8** | **12.6 ± 62.8** | **158.4 ± 62.8** |
| Ronne | 311968 | -78.96 | -65.57 | 0.2 ± 0.4 | 47.2 ± 119.3 | 10.5 ± 119.3 | 21.2 ± 119.9 |
| Filchner | 83304 | -80.56 | -41.02 | 0.4 ± 0.4 | 34.2 ± 29.6 | -1.3 ± 29.6 | 33.5 ± 29.6 |
| **Filchner-Ronne** | **395271** | **–** | **–** | **0.2 ± 0.3** | **81.4 ± 122.9** | **9.2 ± 122.9** | **54.8 ± 123.5** |
| Larsen D | 18282 | -70.72 | -61.64 | 1.8 ± 1.9 | 30.8 ± 31.3 | 3.9 ± 31.3 | 35.3 ± 31.8 |
| Larsen C | 42384 | -67.33 | -63.44 | 2.0 ± 2.5 | 77.9 ± 98.7 | 15.9 ± 98.7 | 64.6 ± 98.8 |
| Larsen B | 1985 | -65.87 | -61.82 | 2.2 ± 2.3 | 3.9 ± 4.2 | 1.6 ± 4.2 | 3.9 ± 4.2 |
| **Larsen** | **75800** | **–** | **–** | **1.6 ± 1.5** | **112.7 ± 103.6** | **21.4 ± 103.6** | **103.8 ± 103.8** |
| **All ice shelves** | **1296230** | **–** | **–** | **1.1 ± 0.1** | **1264.3 ± 147.4** | **160.5 ± 147.4** | **1173.1 ± 148.5** |

**Supplementary Table 1:** Basal melt rates (in m/yr) and meltwater fluxes (in Gt/yr) of ice shelves surveyed in this study. Steady-state mass fluxes can be estimated as the difference between the mean mass flux between 1994 and 2018 and the excess mass flux during the same period. Uncertainties are 95% confidence intervals.